International Journal of Pharmaceutics 654 (2024) 123988

Contents lists available at ScienceDirect

International Journal of Pharmaceutics

journal homepage: www.elsevier.com/locate/ijpharm

Resorbable nanofibrous membranes for local and sustained co-delivery of acyclovir and ketorolac in herpes therapy

Shih-Jyun Shen [a,b], Pin-Chao Feng [a,c], Ren-Chin Wu [d], Yi-Hua Kuo [a], Shih-Jung Liu [a,e,*], Hiroshi Ito [f]

[a] Department of Mechanical Engineering, Chang Gung University, Taoyuan 33302, Taiwan
[b] Department of Anesthesiology, Chang Gung Memorial Hospital-Linkou, Taoyuan 33305, Taiwan
[c] Department of Thoracic and Cardiovascular Surgery, Chang Gung Memorial Hospital at Linkou, Taoyuan 33305, Taiwan
[d] Department of Anatomic Pathology, Linkou Chang Gung Memorial Hospital and Chang Gung University College of Medicine, Taoyuan 33305, Taiwan
[e] Department of Orthopedic Surgery, Bone and Joint Research Center, Chang Gung Memorial Hospital-Linkou, Taoyuan 33305, Taiwan
[f] Graduate School of Organic Materials Science, Yamagata University, Yonezawa, Yamagata 992-8510, Japan

ARTICLE INFO

Keywords:
Herpes
Degradable drug-eluting nanofibers
Electrospinning
Acyclovir
Ketorolac

ABSTRACT

Herpes simplex and herpes zoster are both viral infections caused by members of the herpesvirus family. The former is characterized by painful, fluid-filled blisters or sores on the skin and mucous membranes, while the latter presents as a painful rash with blisters, typically occurring in a single band or patch along one side of the body. The treatment remains a challenge since current antiviral therapy via oral administration may lead to unfavorable side effects such as headaches, nausea, and diarrhea. This study used electrospinning to develop biodegradable nanofibrous poly(lactic-co-glycolic acid) (PLGA) membranes for delivery of both acyclovir and ketorolac. The structure of the spun nanofibers was assessed via scanning electron microscopy (SEM), and the appearance of loaded acyclovir and ketorolac in the nanofibers was confirmed with Fourier-transform infrared spectroscopy (FTIR) and differential scanning calorimetry (DSC). Release profiles of these drugs from the nanofibrous membranes were assessed using in vitro elution studies, high-performance liquid chromatography (HPLC) assays, and in vivo drug release patterns. The electrospun nanofibers had a size range of 283–725 nm in diameter, resembling the extracellular matrix of natural tissue and demonstrated excellent flexibility and extensibility. Notably, the drug-eluting nanofibers exhibited an extended release of high levels of acyclovir and ketorolac over a 21-day period. Thus, biodegradable drug-eluting membranes with a prolonged drug release could be a potential therapeutic approach for treating herpes infections.

1. Introduction

Herpes is caused by the herpes simplex virus (HSV) (Looker et al., 2015, Whitley and Roizman, 2001) , manifesting a variety of symptoms and signs (Whitley and Baron, 1996, Whitley et al., 2007, Strommen et al., 1988, Tunsuriyawong and Puavilai, 2005, Werner and Ghoreschi, 2022) . These symptoms typically involve the development of small blisters or sores in the oral, genital, or anal regions (Nair and Patel, 2023, Patil et al., 2022, Cohen et al., 2013) . The resulting blisters can be intensely painful and may rupture, leaving open sores that can require several weeks to heal. HSV infections contribute significantly to global morbidity, affecting a considerable portion of the population. Herpes is extremely infectious and can be transmitted through direct contact, such as kissing or sexual contact, with an individual who is infected (American Academy of Dermatology Association, Limeres Posse et al., 2017, Schiffer and Corey, 2009) . Within the Herpesviridae family, there are nine distinct viruses that can affect humans. Among these, the most prevalent are HSV-1 and HSV-2, responsible for oral and genital ulcers, respectively (Marchi et al., 2017, Saleh et al., 2023, Mathew and Sapra, 2023) . Additionally, the varicella-zoster virus (VZV) can infect individuals, resulting in herpes zoster commonly known as shingles. Shingles are characterized by a painful rash that typically appears on one side of the body, often in a band-like pattern. Following a shingles infection, the virus establishes a latent presence in neurons. Over time, VZV can reactivate, causing herpes zoster, characterized by the development of painful vesicles and the potential for lifelong chronic

* Corresponding author at: Biomaterials Lab, Mechanical Engineering, Chang Gung University, 259, Wen-Hwa 1st Road, Kwei-San, Tao-Yuan 33302, Taiwan.
E-mail address: shihjung@mail.cgu.edu.tw (S.-J. Liu).

https://doi.org/10.1016/j.ijpharm.2024.123988
Received 25 October 2023; Received in revised form 21 February 2024; Accepted 8 March 2024
Available online 11 March 2024

neuralgic pain (Patil et al., 2022, Koshy et al., 2018) .

While herpes simplex and herpes zoster cannot be cured, treatments are accessible to help manage the symptoms and decrease the frequency and intensity of outbreaks (Modi et al., 2008), and the therapeutic approach for herpes zoster uses antiviral agents and symptom-relieving medication (Bader, 2013, Opstelten et al., 2008) . Currently the use of antiviral medications (e.g., acyclovir, valacyclovir, and famciclovir) remain the most common and effective treatments for herpes. These drugs can help decrease the severity and duration of symptoms and he frequency of outbreaks. However, the antiviral therapy via oral administration may induce unfavorable side effects such as headaches, nausea, and diarrhea (Kimberlin et al., 2007). Additionally, extended systemic use of antiviral treatment can also contribute to the emergence of drug-resistant viral strains, posing challenges in their effective treatment (Strasfeld and Chou, 2010). On the other hand, various analgesic agents with distinct routes of administration are used to attenuate the tingling pain linked to herpes zoster infection. Nonetheless, the efficacy of these agents is limited by their relatively short duration of action, necessitating multiple administrations throughout the course of the disease (Opstelten et al., 2008, Jung and Park, 2016, Johnson et al., 2010) . Hence, there is a need for novel therapies capable of overcoming these limitations. A promising strategy involves employing degradable drug-eluting implants for the localized and sustained delivery of antiviral drugs and analgesic agents to the targeted site. By implanting these devices at the dermatome where the varicella rash develops, near the dorsal roots of the spinal cord, we can not only tackle the varicella-zoster virus emanating from the dorsal root ganglia but also address the intense neuralgic pain associated with the varicella rash in that dermatome. This approach offers simultaneous analgesic, anti-inflammatory and antiviral effects.

Ideally, an implant for herpes treatment should give high concentrations of an antiviral drug to the target site over a period of days to weeks. An implant should offer sustained analgesic relief locally to decrease pain. It should emulate the morphological and biological function of native extracellular matrix (ECM) proteins that support and regulate cellular activities. Additionally, the implant should be resorbable after fulfilling its function and biocompatible, ensuring that its decomposition does not cause any tissue irritation. However, an optimal combination of designs and materials to provide such a durable and biocompatible implant for treating of herpes has not yet been established.

Herein, we used electrospinning technology to develop a resorbable nanofibrous poly(lactic-co-glycolic acid) (PLGA) implant to simultaneously deliver acyclovir and ketorolac, employing the electrospinning technology. Differing from the antiviral acyclovir, ketorolac is a nonsteroidal anti-inflammatory drug (NSAID) used for short-term relief of inflammation, moderate to severe pain, and fever (Brocks and Jamali, 1992, Buckley and Brogden, 1990) .

PLGA is an aliphatic polymer comprising a polyester backbone that is created by copolymerizing monomers of lactic and glycolic acid (Hines and Kaplan, 2013, Lee et al., 2018, Gentile et al., 2014) . Depending on the composition of these monomers, the crystallinity, hydrophilicity, and glass transition temperature (typically between 40 and 60 °C) of the copolymer can vary (Liu and McEnnis, 2022, Swider et al., 2018, Lu et al., 2023) . PLGA is both bioresorbable and biocompatible, offering a broad spectrum of degradation durations and tunable properties, and consequently has been extensively studied for its potential in the managed discharge of drugs, proteins, and other biomolecules (Wang et al., 2020). Electrospinning is an electrohydrodynamic technique where an electrically charged liquid droplet is used to produce a jet, which is then stretched and elongated to create fibers. (Xue et al., 2019, Villarreal-Gómez et al., 2016, Sill and von Recum, 2008, Casanova et al., 2018, Partheniadis et al., 2022) . During electrospinning, a liquid is extruded from a spinneret to form a suspended droplet caused by the surface tension. When an electric charge is applied, the surface of the liquid is charged with the same polarity and experiences electrostatic repulsion, causing the droplet to transform into a structure known as a Taylor cone, from which a charged jet is emitted. Initially, the jet travels in a straight trajectory but soon experiences significant whipping motions due to bending instabilities. With continued stretching, the jet rapidly solidifies, producing an accumulation of extended fibers onto a grounded collector.

Following electrospinning of PLGA with acyclovir and ketorolac, the morphological characteristics of the produced nanofibers were evaluated via scanning electron microscopy (SEM). Fourier-transform infrared spectroscopy (FTIR) and differential scanning calorimetry (DSC) analyses and to confirm the presence of loaded acyclovir and ketorolac within the nanofibers. The release kinetics of these pharmaceuticals from the nanofibrous membranes were studied through elution techniques and analyzed by high-performance liquid chromatography (HPLC) assays, and in vivo elution profiles were evaluated in a rat subcutaneous model. Furthermore, the concentrations of the drugs in the bloodstream were measured to evaluate the systemic absorption of the drugs.

2. Materials and method

2.1. Degradable polymer, solvent and drugs

The degradable polymer used in this study was PLGA (LA:GA ratio of 50:50, 33 kDa), the solvent used for electrospinning PLGA was Hexafluoroisopropanol (HFIP), and the drugs used were acyclovir and ketorolac. All materials were acquired from Sigma-Aldrich (Saint Louis, MO, USA), a reputable supplier of research materials.

2.2. Preparation of pristine PLGA and drug-eluting PLGA nanofibrous mats

Drug-loaded nanofibrous implants were prepared with 105.6 mg of acyclovir, 105.6 mg of ketorolac, and 628.8 mg of PLGA and were mixed with 3 mL of HFIP. The resulting solution was then electrospun using a custom-built spinning apparatus (Hsu et al., 2023), with a voltage of 17 kV, a flow rate of 0.6 mL/h, and a distance of 15 cm between the needle and the collection plate. All spinning tests were performed at ambient temperature. The thickness of the nanofibers was approximately 0.11 mm. The preparation of pristine PLGA nanofibrous mats followed the same procedure, except that 840 mg of PLGA was mixed with 3 mL of HFIP. To eliminate any remaining solvent, all electrospun membranes were placed under vacuum drying conditions at 40 °C for 72 h. Dried fibers were stored at a temperature of 4 °C until use.

2.3. Tensile strength of spun nanofibers

The mechanical properties of the fabricated nanofibrous mats (Partheniadis et al., 2022), including tensile strength (MPa) and elongation at breakage (%), were assessed with a Lloyd tensiometer (Ametek, Berwyn, PA, USA). A membrane strip measuring 10 mm x 50 mm x 0.11 mm was sliced from the electrospun nanofibrous mat, secured between two clamps, and drawn by the upper clamp over a distance of 15 cm before being returned to its initial position. The tensile strength and elongation at breakage were calculated as follows.

$$\text{Tensile strength (MPa)} = \text{Breaking force (N)}/\text{Cross-sectional area of sample (mm}^2) \quad (1)$$

$$\text{Elongation at breakage } (\%) = \text{Increase in length at breaking point (mm)/Original length (mm)} \times 100\% \quad (2)$$

2.4. Microscopic evaluation

The structure of electrospun nanofibers loaded with drugs was examined using SEM (FESEM, JEOL JSM-7500F, Tokyo, Japan) after being coated with a layer of gold. The size distribution of spun nanofibers was determined by evaluating 50 randomly selected fibers.

2.5. Hydrophobicity

The hydrophobicity of virgin PLGA nanofibers with and without drugs was assessed with a water contact angle analyzer (First Ten Angstroms, USA). Pure distilled water was administered onto the surface of the samples in a controlled manner, and the wetting angles were evaluated with a video monitor. Experiments were repeated three times to ensure reliability and consistency of the results.

2.6. Hydrogen-1 nuclear magnetic resonance

Hydrogen-1 nuclear magnetic resonance (1H NMR) spectrometry was used to analyze the spectra of drug-embedded PLGA nanofibers with a Bruker AV III HD 600 MHz NMR spectrometer (Billerica, MA, USA) in the range + 16 to −4 ppm. The NMR spectra were recorded in solution, with deuterated chloroform serving as the solvent.

2.7. Thermal analysis

The thermal characteristics of both pristine PLGA and PLGA nanofibers loaded with drugs were examined employing a TA-DSC25 differential scanning calorimeter (DSC) from TA Instruments in New Castle, DE, USA. Nitrogen served as the selected gas for the analysis, and the data were processed using the built-in software. The scanning temperature spanned from 30 °C to 250 °C, and the nanofibrous samples underwent heating at a rate of 10 °C per minute.

2.8. In vitro release

The discharge characteristic of acyclovir and ketorolac from spun nanofibers was assessed through an in vitro elution technique, a laboratory approach to studying the controlled release of substances, especially drugs, from different formulations or delivery systems (Lee et al., 2022; Weng et al., 2022). Nanofibrous samples were individually placed into glass test tubes (N = 3), with each tube containing 1 mL of phosphate buffer saline (PBS) and were then incubated at 37 °C for 24 h, following which the eluent was removed and analyzed. Fresh PBS (1 mL) was used to replenish the sample, and the process was repeated over a 30-day course. The concentration of the pharmaceuticals in collected eluents was estimated via a HPLC assay, which was perofrmed on a Hitachi L-2200R multi-solvent delivery system (Hitachi High-Technologies Corporation, Tokyo, Japan). Each experiment was conducted three times.

2.9. In vivo animal test

This study used Sprague-Dawley rats (weighing 375 ± 25 g each). The experimental protocols involving the use of animal subjects adhered to the guidelines and rules of the National Institute of Health of Taiwan and were supervised by a licensed veterinarian. The Institutional Animal Care and Use Committee of Chang Gung University granted approval for all animal-related procedures (IACUC Approval No.: CGU111-016).

A 5-cm incision was created at the back of each animal Fig. 1). After the implantation of the drug-loaded nanofibers (10 mm × 50 mm), the wound was sutured shut with 3–0 Vicryl sutures. At various time points (1, 3, 7, and 14 days) post-implantation, tissue samples from areas

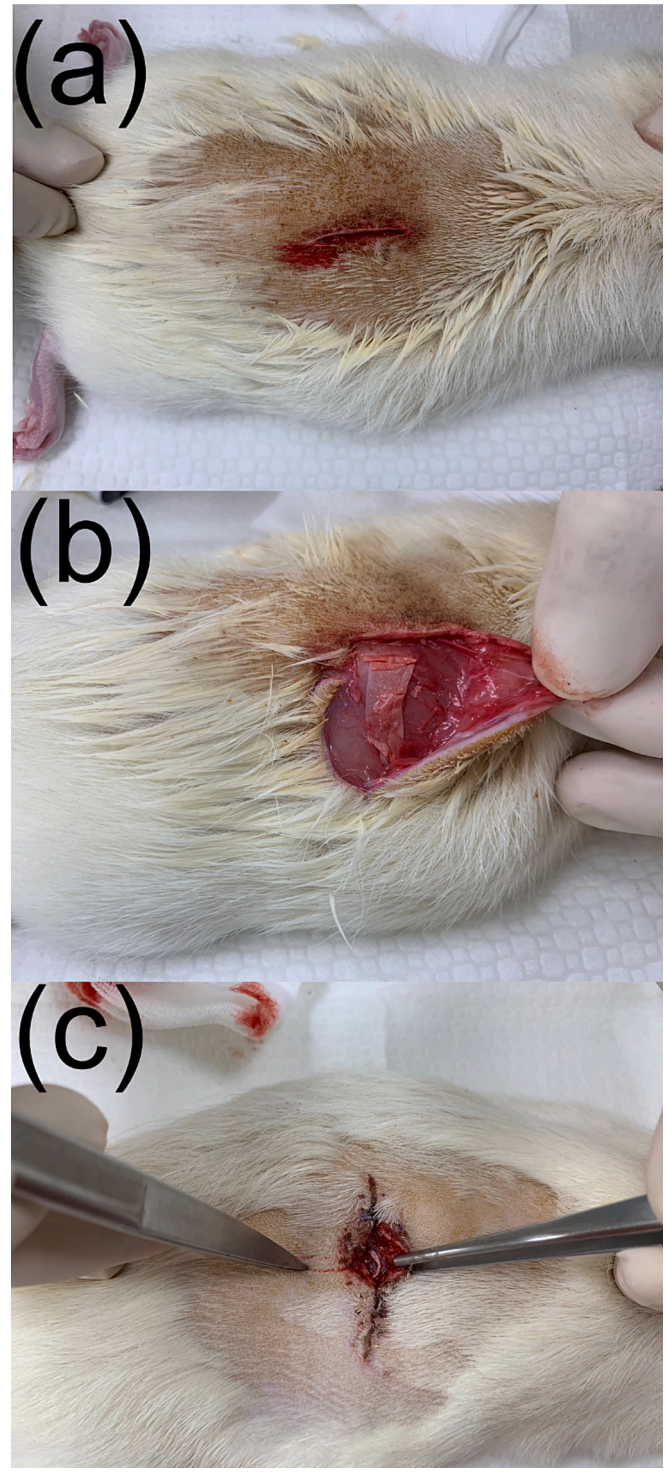

Fig. 1. Surgical procedure for in vivo test. (a) An incision was made on the back of the rat; (b) implantation of the drug-loaded nanofibers; and (c) suturing of the wound.

surrounding the implanted nanofibers were collected. HPLC assays were used to measure the drug concentrations within the collected tissue samples. Blood draws were performed on post-implantation days 1 and 3 to measure the drug concentration in the blood. Additionally, histological analyses were performed on tissue samples collected on days 1, 3, 7 and 14 after the operation for hematoxylin and eosin (H&E) staining.

2.10. Statistical analysis

Experimental data are shown as the mean value ± standard deviation. Paired t-tests were conducted to determine statistical differences between groups. Statistical significance was characterized as a p-value less than 0.05. The data were analyzed using SPSS software (version 17.0 for Windows; SPSS Inc., Chicago, Illinois, USA).

3. Results

3.1. Assessment of drug-eluting nanofibers

The morphology and diameter distribution of both pristine and drug-loaded PLGA nanofibers are shown in Fig. 2. The size compositions of pristine and drug-loaded PLGA nanofibers were estimated to be 728.5 ± 248.2 nm and 283.6 ± 72.4 nm in diameter, respectively. The incorporation of pharmaceuticals significantly reduced in the size of the electrospun fibers ($p < 0.05$). The presence of drugs in the nanofibers decreased the PLGA content in the fibers, rendering them less resistant to the electric stretching force experienced in the axial direction during electrospinning. Consequently, the dimension of electrospun fibers diminished proportionally. Moreover, the significant deviation in fiber size distribution could be attributed to suboptimal process parameters, such as the concentration of PLGA in the solution, the volumetric flow rate of the PLGA solution, the distance traveled between the needle and the ground collection, the positive voltage applied to polymer solutions, and the type of solvent utilized (Chen et al., 2019). Additional work will be needed to optimize the electrospinning process to reduce the size deviation of nanofibers.

The contact angles of pristine and drug-loaded PLGA nanofibers were 135.6 ± 3.4° and 95.5 ± 4.7°, respectively (Fig. 3). The incorporation of acyclovir and ketorolac substantially enhanced the hydrophilicity of the spun nanofibrous implants ($p < 0.05$).

The mechanical properties of both pristine PLGA and drug-loaded PLGA nanofibrous membranes are shown in Fig. 4. The average tensile strengths for nanofibrous membranes with pristine PLGA and drug-loaded PLGA were approximately 3.24 ± 0.56 MPa and 2.38 ± 0.09 MPa, respectively ($p > 0.05$). The nanofibers within the pristine PLGA showed greater strength and elongation at breakage (147.9 ± 57.5 %) compared with those within the drug-loaded PLGA (43.6 ± 2.6 %) ($p < 0.01$). In drug-loaded polymeric composites, the polymer serves as the primary component to resist external forces and provide plastic extension. The inclusion of acyclovir and ketorolac within the composite reduced the PLGA content, which decreased the mechanical strengths and elongation during electrospinning of nanofibers.

The 1H NMR spectra of drug-loaded PLGA nanofibers are shown in Fig. 5a. The peak at 2.1 ~ 3.0 ppm was caused by the C-N bonds of the loaded acyclovir. The new peak at 2.5 ~ 3.0 ppm was resulted from the NH bond of embedded acyclovir and ketorolac (Aiello et al., 2022, Świerzewski et al., 2002) . Fig. 5b shows the thermogram of pristine PLGA and drug-loaded PLGA nanofibers. The exothermal peak near 171.9 °C that corresponds to acyclovir (Hassan et al., 2020) and the peaks at 132.4, and 258.3 °C attributable to ketorolac (Sohn and Seo, 2004) diminished after the drugs were embedded into the polymer matrix. These assays collectively confirm the successful integration of pharmaceuticals within the PLGA nanofibers.

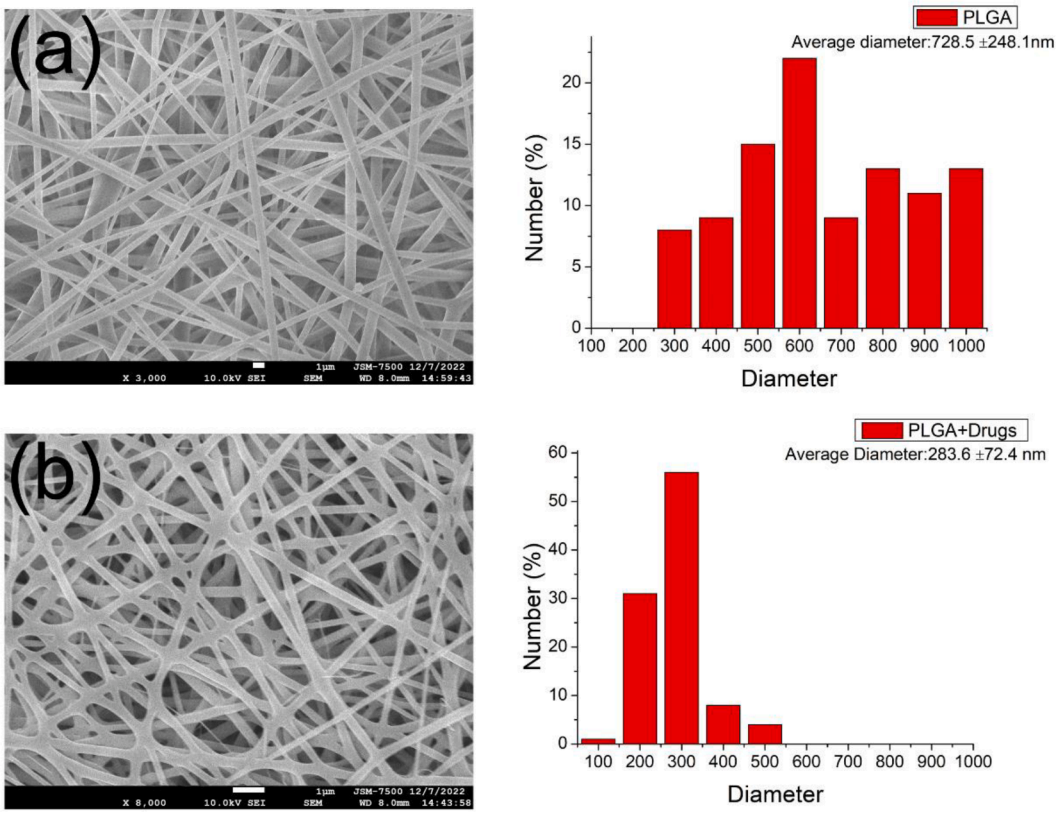

Fig. 2. SEM images and fiber particle size distribution of electrospun (a) pristine PLGA nanofibers and (b) drug-loaded PLGA nanofibers.

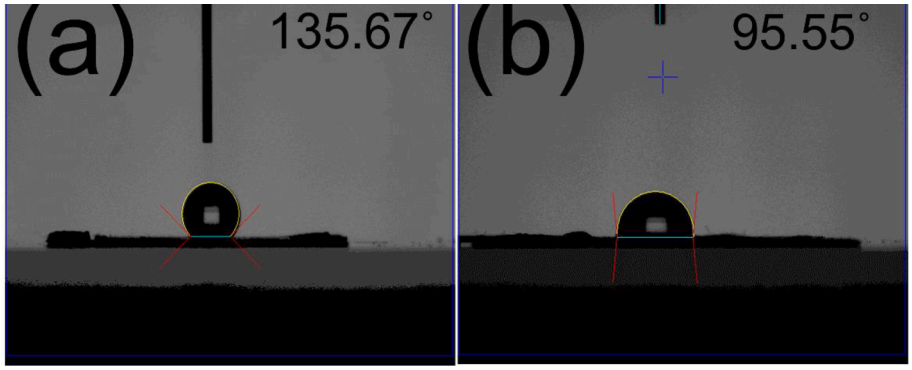

Fig. 3. Water contact angles of (a) pristine PLGA and (b) drug-loaded PLGA nanofibers.

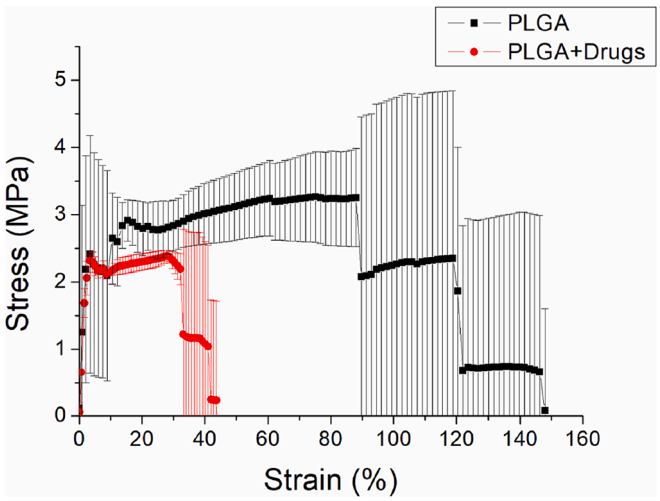

Fig. 4. Tensile curves of pritine and drug-loaded PLGA nanofibers.

3.2. *In vitro and in vivo release*

The daily and accumulated in vitro release patterns of acyclovir and ketorolac, from the nanofibers is shown in Fig. 6. Both drugs showed a burst release at day one. The discharge curves of ketorolac then displayed a near-linear gradual discharge for 21 days. Acyclovir, on however, displayed a peak discharge at 11 days, followed by a steady and decreasing elution over 21 days. Overall, the drug-loaded nanofibers enabled prolonged discharge of high drug concentrations for over 21 days in vitro.

The drug elution patterns in the tissue and blood are illustrated in Fig. 7. The nanofibers sustained the release of high levels of acyclovir and ketorolac for more than 21 days in rat tissues with comparatively lower levels present in the blood.

3.3. *Histology assay*

The histological examination of muscle cross-sections adjacent to the biomaterial membrane was conducted at postoperative days 1, 3, 7, and 14 (Fig. 8). Notably, the presence of leukocytes (indicated by blue staining within the muscle layer) was observed on postoperative days 1 and 3, with their numbers gradually declining by postoperative day 7. By postoperative day 14, only a minimal population of leukocytes was discernible, indicating a resolution of the inflammatory response. Crucially, no histological evidence of tissue necrosis was observed during the examination.

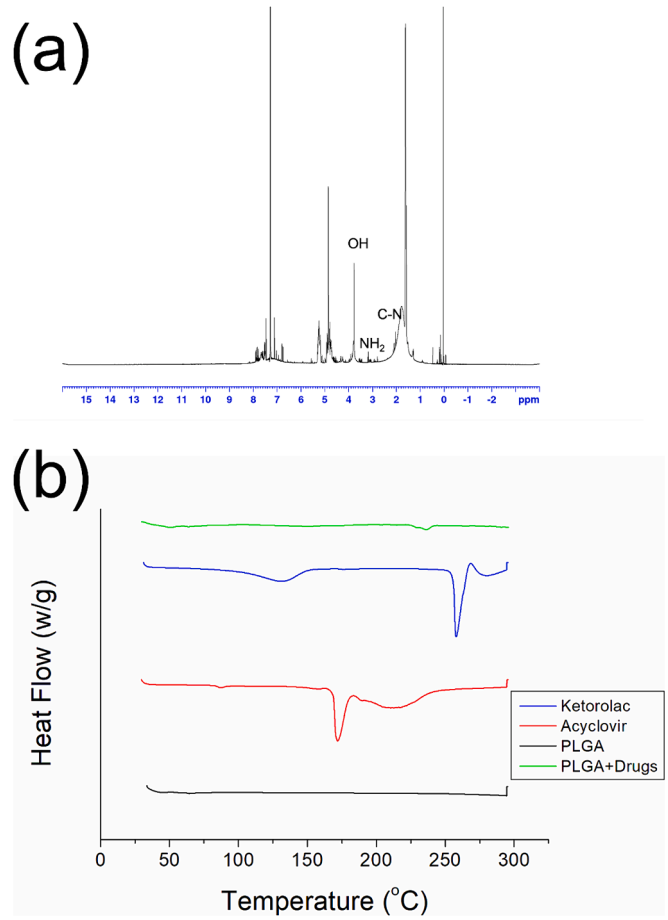

Fig. 5. (a) 1H NMR spectra and (b) DSC thermograms of pristine and drug-loaded PLGA nanofibers.

4. Discussion

Degradable polymer can serve as a novel drug delivery system to modulate drug properties and extend their duration of action. This approach has potential in enhancing the efficacy of antiviral and analgesic drugs for herpes zoster treatment. The aqueous solubility of acyclovir is reported to be inadequate, leading to limited absorption (Bruni et al., 2013, Shamshina et al., 2017) . Liu et al. (Liu et al., 2014) proposed a new strategy to tackle this issue for inadequately water-soluble drugs in equally poorly water-soluble environments. They achieved this by employing polyvinylpyrrolidone (PVP) as a hydrophilic polymer matrix through coaxial electrospraying to create core–shell

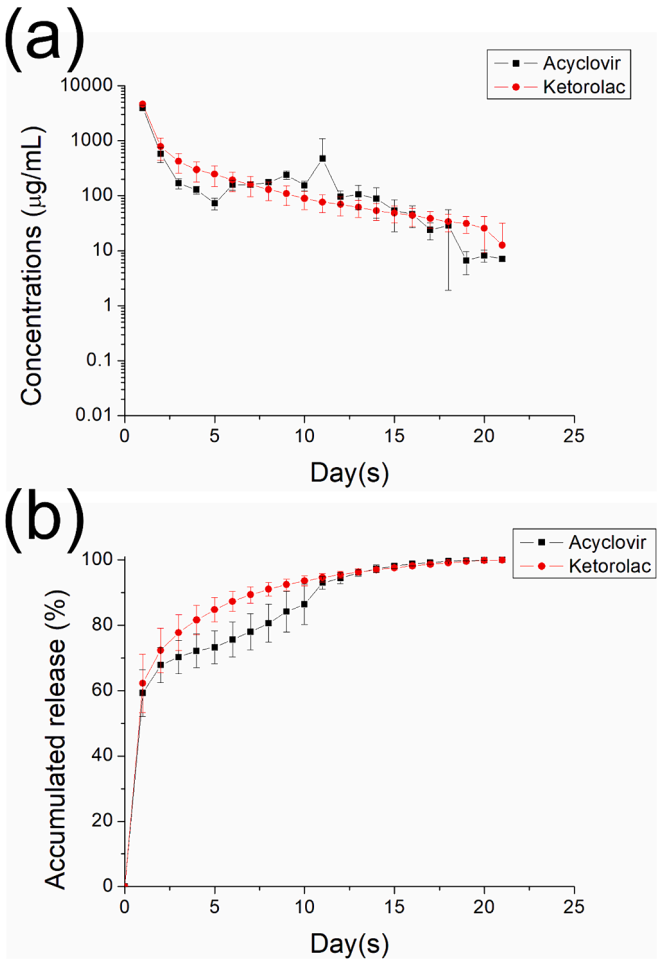

Fig. 6. In vitro (a) daily and (b) cumulative release of acyclovir and ketorolac.

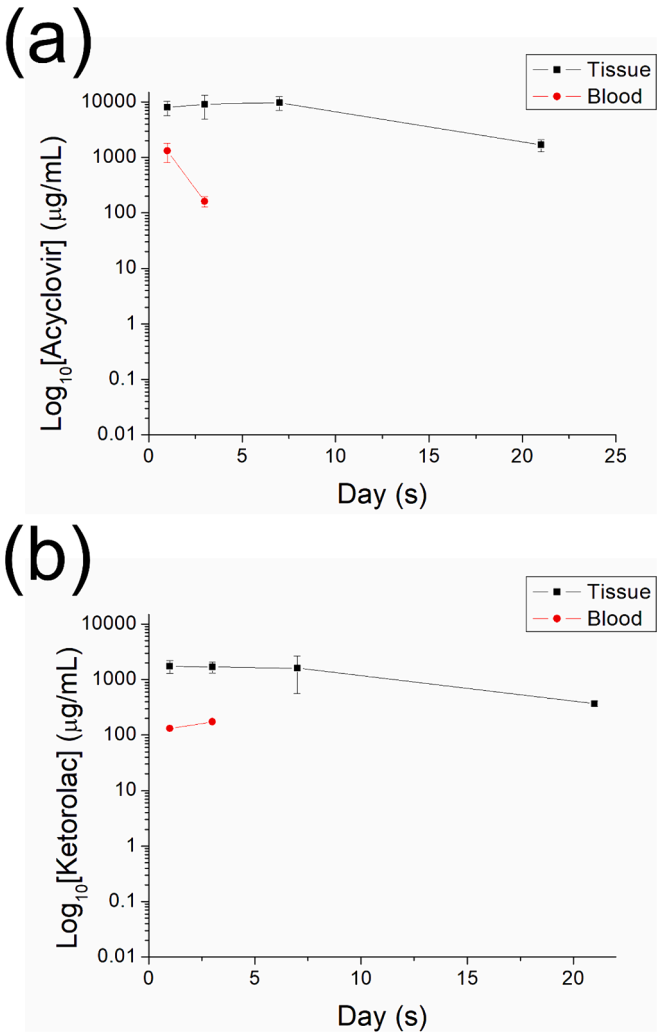

Fig. 7. In vivo elution of acyclovir and ketorolac from nanofibers.

solid dispersions of acyclovir. The resulting core–shell microparticles with tunable drug contents demonstrated a significant improvement in the solubility of acyclovir as shown by the enhanced dissolution and permeation performance.

In view of the limited bioavailability and short duration of action of oral acyclovir, Dhaliwal et al. (Dhaliwal et al., 2008) assessed the applicability of mucoadhesive microspheres in the gastroretentive delivery of acyclovir and explored the use of mucoadhesive polymers such as chitosan, thiolated chitosan, Carbopol 71G, and Methocel K15M. Their results showed prolonged drug delivery for 24 h, as compared with that at 5 h after administration of drug in solution form in the upper GI tract. Bhosale et al. (Bhosale et al., 2011) formulated polymeric nanodrug delivery systems for acyclovir with mucoadhesive properties. They used PLGA as the polymer, polycarbophil (Noveon AA-1) as the mucoadhesive component, and pluronic F68 as a stabilizing agent. Acyclovir-loaded mucoadhesive PLGA nanoparticles were effective in extending drug discharge for over 30 h. Costa et al. (Costa et al., 2019) developed a dual acyclovir and omega-3 fatty acid loaded fibrous mat that provided an extended discharge of acyclovir for 96 h and enhanced the ability of the drug to permeate the skin.

Effective management of pain is crucial for resolving herpes zoster infection, in addition to antiviral therapy. Non-steroidal anti-inflammatory drugs (NSAIDs) have been shown to be effective as analgesic agents for reducing the painful sensation associated with the condition. Compared with local anesthetics, NSAIDs have a wider range of pain-relieving properties. Previous studies (Fraser-Smith and Matthews, 1988, Romanowski and Gordon, 2001) reported that the use of ketorolac did not affect the efficacy of antiviral agents. Therefore, NSAIDs, including ketorolac, are a safe and effective option for the therapy of herpes zoster-associated pain.

Herein, we successfully applied the electrospinning technique to develop resorbable nanofibrous membranes that provided local and prolonged discharge of antiviral agents for infection control and analgesics for pain relief post-surgery. Our results confirm that the drug-embedded nanofibers exhibit an extended discharge of high levels of acyclovir and ketorolac over 21 days, which is beneficial for preventing infection and manage pain. The nanofibers also displayed excellent flexibility and favorable biocompatibility, thus facilitating implantation. Moreover, hydrophilic environments can generally attract and retain water, creating a milieu conducive to the dissolution and availability of nutrients essential for cell proliferation. The inclusion of acyclovir and ketorolac heightened the hydrophilicity of the PLGA nanofibrous mats, thereby further improving tissue healing. This discovery suggests that resorbable nanofibers containing these drugs can function as a viable scaffold for treating herpes.

Local pharmaceutical delivery to the target tissue provides several advantages over systemic drug delivery, including high drug levels at the site of action, minimized systemic exposure, improved efficacy, reduced dosing frequency, and targeted delivery, and is therefore an important tool for treating a wide range of diseases. Generally, the release of drugs from a polymer-based delivery vehicle can be segmented into three stages: initial burst, diffusion-based release, and degradation-driven release. After the electrospinning process, most of the pharmaceuticals are evenly spread throughout the nanofiber matrix,

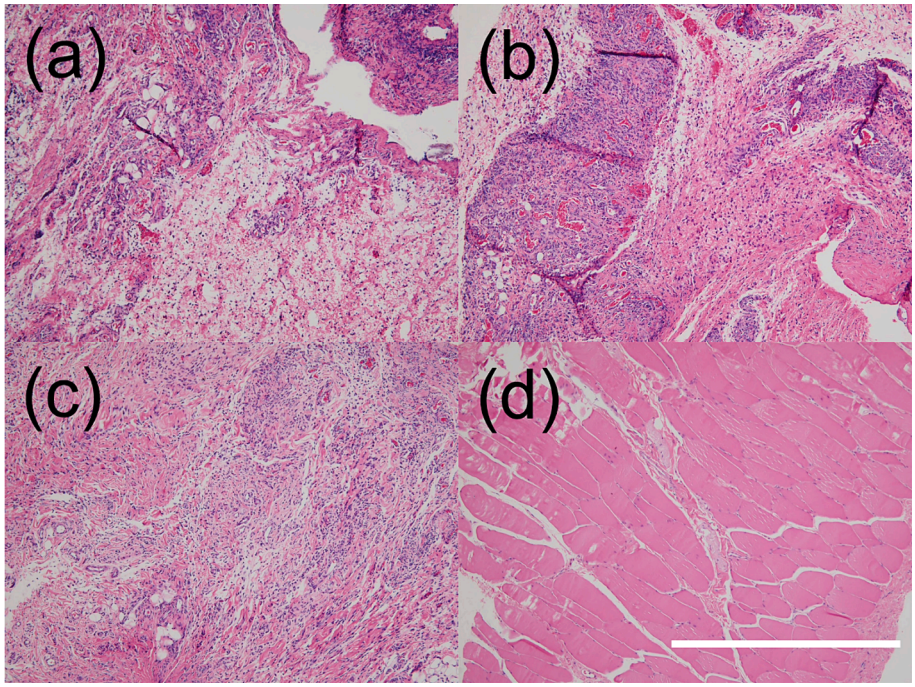

Fig. 8. Postoperative histological staining at (a) 1, (b) 3, (c) 7, and (d) 14 days. The intensity of blue staining, indicative of leukocytes within the muscle tissue, exhibited a gradual decline and was nearly absent by day 14. Additionally, no discernible evidence of tissue necrosis was observed. (Scale bar = 1 mm). (For interpretation of the references to colour in this figure legend, the reader is referred to the web version of this article.)

with surface-bound drugs experiencing an initial burst release at day one. Thereafter, the regulation of drug discharge is influenced by the combined processes of polymer degradation and simultaneous drug diffusion. Additionally, the solubility of a drug in a nanofiber matrix determines how well it dissolves or disperses within the structure. Higher solubility can enhance drug release, promoting controlled and sustained delivery. However, extremely high solubility may lead to a burst release if the drug rapidly dissolves upon contact with the surrounding environment. The adopted drugs exhibit good solubility with the solvent and can be evenly distributed in the polymeric matrix, resulting in a uniformly diminishing release post the initial burst. Permeability refers to a drug's ability to move through the nanofiber matrix. The porous structure of spun nanofibrous mats allows for good permeability and enhanced drug diffusion, leading to a steady and gradually decreasing discharge of drugs from the nanofibers.

In addition, the nanofibers produced higher drug concentrations in vivo over an extended time compared with those observed in vitro. This could be due to the lower metabolic activity in vivo compared with the drug release observed in the in vitro PBS environment. Consequently, the drug levels in vivo remained elevated throughout the 21-day study period.

Due to the limited oral bioavailability of Acyclovir, which ranges between 10 and 20 %, frequent dosing of five times per day is necessitated. This regimen presents inherent challenges, including inconvenience and the propensity for patient non-adherence, thereby compromising therapeutic efficacy. While most previous literature has primarily focused on modifying the absorption of acyclovir through biomedical materials, our experiment is the first to combine acyclovir—an antiviral drug—with the analgesic and anti-inflammatory medication ketorolac, implanted at the site of herpesvirus infection. Additionally, patients under herpesvirus infection endure severe neurological pain during the initial disease stages. The adoption of a sustained-release implant system for controlled and continuous drug delivery offers a pragmatic solution, markedly improving dosing convenience. Moreover, the adjunctive use of ketorolac augments the regimen by conferring analgesic and anti-inflammatory effects, enhancing the overall treatment approach.

This preliminary work had some limitations. First, a non-herpes animal model was used, which may restrict a more general interpretation of the results. Further research will also be necessary to optimize the drug doses loaded into the resorbable membranes and to reduce the size distribution of spun nanofibers. Furthermore, the applicability of our findings to human herpes infection remains uncertain and warrants further investigation. These areas will be addressed in our future research endeavors.

5. Conclusions

We used electrospinning technology to develop biodegradable nanofibrous PLGA membranes that could locally deliver acyclovir and ketorolac. Our results revealed that the electrospun nanofibers had a size range of 283 to 725 nm, similar to that of the extracellular matrix of natural tissue and exhibited excellent flexibility and extensibility. The drug-eluting nanofibers also demonstrated extended release of high levels of acyclovir and ketorolac over a 14-day period. The study demonstrates that these biodegradable drug-eluting membranes with prolonged drug release hold promise as a potential therapeutic approach for treating herpes infections.

Funding

The financial supports of the Ministry of Science and Technology, Taiwan (Contract No. 111-2221-E-182-004-MY3 and 111-2221-E-182-005-MY2) and Chang Gung Memorial Hospital (Contract No. CMRPD2M0132) for this research are gratefully acknowledged.

CRediT authorship contribution statement

Shih-Jyun Shen: Writing – original draft, Resources, Project administration, Methodology, Investigation, Data curation, Conceptualization. **Pin-Chao Feng:** Validation, Methodology, Investigation, Formal analysis, Data curation, Conceptualization. **Ren-Chin Wu:**

Visualization, Validation, Supervision, Methodology, Formal analysis. **Yi-Hua Kuo:** Software, Methodology, Investigation, Formal analysis, Data curation. **Shih-Jung Liu:** Writing – review & editing, Visualization, Validation, Supervision, Software, Resources, Methodology, Investigation, Funding acquisition, Formal analysis. **Hiroshi Ito:** Validation, Project administration, Methodology, Investigation, Formal analysis, Conceptualization.

Declaration of competing interest

The authors declare that they have no known competing financial interests or personal relationships that could have appeared to influence the work reported in this paper.

Data availability

Data will be made available on request.

References

Aiello, F., Ucccello-Barretta, G., Picchi, C., Nazzi, S., Recchimurzo, A., Balzano, F., 2022. NMR investigation of the interaction of three non-steroidal anti-inflammatory drugs with human serum albumin. Molecules 27 (19), 6647. https://doi.org/10.3390/molecules27196647.

American Academy of Dermatology Association. Herpes Simplex: Overview. (https://www.aad.org/public/diseases/a-z/herpes-simplex-overview) Accessed 5/17/2022.

Bader, M.S., 2013. Herpes zoster: diagnostic, therapeutic, and preventive approaches. Postgrad. Med. 125 (5), 78–91. https://doi.org/10.3810/pgm.2013.09.2703.

Bhosale, U., Kusum, D.V., Jain, N., 2011. Formulation and optimization of mucoadhesive nanodrug delivery system of acyclovir. J. Young Pharmacists : JYP 3 (4), 275–283. https://doi.org/10.4103/0975-1483.90236.

Brocks, D.R., Jamali, F., 1992. Clinical pharmacokinetics of ketorolac tromethamine. Clin. Pharmacokinet. 23 (6), 415–427. https://doi.org/10.2165/00003088-199223060-00003.

Bruni, G., Maietta, M., Maggi, L., Mustarelli, P., Ferrara, C., Berbenni, V., Milanese, C., Girella, A., Marini, A., 2013. Preparation and physicochemical characterization of acyclovir cocrystals with improved dissolution properties. J. Pharm. Sci. 102 (11), 4079–4086. https://doi.org/10.1002/jps.23721.

Buckley, M.M., Brogden, R.N., 1990. Ketorolac. a review of its pharmacodynamic and pharmacokinetic properties, and therapeutic potential. Drugs 39 (1), 86–109. https://doi.org/10.2165/00003495-199039010-00008.

Casanova, M.R., Reis, R.L., Martins, A., Neves, N.M., 2018. The use of electrospinning technique on osteochondral tissue engineering. Adv. Exp. Med. Biol. 1058, 247–263. https://doi.org/10.1007/978-3-319-76711-6_11.

Chen, Y.P., Liu, H.Y., Liu, Y.W., Lee, T.Y., Liu, S.J., 2019. Determination of electrospinning parameters' strength in poly(D, L)-lactide-co-glycolide micro/nanofibers diameter tailoring. J. Nanomater. 2019, 2626085.

Cohen, K.R., Salbu, R.L., Frank, J., Israel, I., 2013. Presentation and management of herpes zoster (shingles) in the geriatric population. P & T: a Peer-Reviewed J. Formulary Manage. 38 (4), 217–227.

Costa, T., Ribeiro, A., Machado, R., Ribeiro, C., Lanceros-Mendez, S., Cavaco-Paulo, A., Almeida, A., das Neves, J., Lúcio, M., Viseu, T., 2019. Polymeric electrospun fibrous dressings for topical co-delivery of acyclovir and Omega-3 fatty acids. Front. Bioeng. Biotechnol. 7, 390. https://doi.org/10.3389/fbioe.2019.00390.

Dhaliwal, S., Jain, S., Singh, H.P., Tiwary, A.K., 2008. Mucoadhesive microspheres for gastroretentive delivery of acyclovir: in vitro and in vivo evaluation. AAPS J. 10 (2), 322–330. https://doi.org/10.1208/s12248-008-9039-2.

Fraser-Smith, E.B., Matthews, T.R., 1988. Effect of ketorolac on herpes simplex virus type one ocular infection in rabbits. J. Ocul. Pharmacol. 4 (4), 321–326. https://doi.org/10.1089/jop.1988.4.321.

Gentile, P., Chiono, V., Carmagnola, I., Hatton, P.V., 2014. An overview of poly(lactic-co-glycolic) acid (PLGA)-based biomaterials for bone tissue engineering. Int. J. Mol. Sci. 15 (3), 3640–3659. https://doi.org/10.3390/ijms15033640.

Hassan, H., Bello, R.O., Adam, S.K., Alias, E., Meor Mohd Affandi, M.M.R., Shamsuddin, A.F., Basir, R., 2020. Acyclovir-loaded solid lipid nanoparticles: optimization, characterization and evaluation of its pharmacokinetic profile. Nanomaterials (basel, Switzerland) 10 (9), 1785. https://doi.org/10.3390/nano10091785.

Hines, D.J., Kaplan, D.L., 2013. Poly(lactic-co-glycolic) acid-controlled-release systems: experimental and modeling insights. Crit. Rev. Ther. Drug Carrier Syst. 30 (3), 257–276. https://doi.org/10.1615/critrevtherdrugcarriersyst.2013006475.

Hsu, Y.H., Yu, Y.H., Chou, Y.C., Lu, C.J., Lin, Y.T., Ueng, S.W., Liu, S.J., 2023. Sustained release of antifungal and antibacterial agents from novel hybrid degradable nanofibers for the treatment of polymicrobial osteomyelitis. Int. J. Mol. Sci. 24 (4), 3254. https://doi.org/10.3390/ijms24043254.

Johnson, R.W., Bouhassira, D., Kassianos, G., Leplège, A., Schmader, K.E., Weinke, T., 2010. The impact of herpes zoster and post-herpetic neuralgia on quality-of-life. BMC Med. 8, 37. https://doi.org/10.1186/1741-7015-8-37.

Jung HY, Park HJ. (2016). Pain Management of Herpes Zoster. InTech, 2016. https://www.intechopen.com/chapters/50380.

Kimberlin, D.W., Whitley, R.J., 2007. Antiviral therapy of HSV-1 and -2. In: Arvin, A., Campadelli-Fiume, G., Mocarski, E. (Eds.), Human Herpesviruses: Biology, Therapy, and Immunoprophylaxis. Cambridge University Press, Cambridge. Chapter 64. Available from:

Koshy, E., Mengting, L., Kumar, H., Jianbo, W., 2018. Epidemiology, treatment and prevention of herpes zoster: a comprehensive review. Indian J. Dermatol. Venereol. Leprol. 84 (3), 251–262. https://doi.org/10.4103/ijdvl.IJDVL_1021_16.

Lee, D.M., Hsu, M.Y., Li, M.J., Liu, Y.W., Liu, S.J., Liu, C.Y., Hiroshi, I., 2018. Factors affecting the co-axial electrospraying of core-shell-structured poly(D, L-lactide-co-glycolide) microparticles. Jpn J Appl Phys 57, 116702.

Lee, C.H., Huang, C.H., Hung, K.C., Huang, S.C., Kuo, C.C., Liu, S.J., 2022. Nanofibrous vildagliptin/PLGA membranes accelerate diabetic wound healing by angiogenesis. Pharmaceuticals 15, 1358.

Limeres Posse, J., Diz Dios, P., & Scully, C. (2017). Viral Diseases Transmissible by Kissing. Saliva Protection and Transmissible Diseases, 53–92. DOI: 10.1016/B978-0-12-813681-2.00004-4.

Liu, Z.P., Cui, L., Yu, D.G., Zhao, Z.X., Chen, L., 2014. Electrosprayed core-shell solid dispersions of acyclovir fabricated using an epoxy-coated concentric spray head. Int. J. Nanomed. 9, 1967–1977. https://doi.org/10.2147/IJN.S59516.

Liu, G., McEnnis, K., 2022. Glass transition temperature of PLGA particles and the influence on drug delivery applications. Polymers 14 (5), 993. https://doi.org/10.3390/polym14050993.

Looker, K.J., Magaret, A.S., Turner, K.M., Vickerman, P., Gottlieb, S.L., Newman, L.M., 2015. Global estimates of prevalent and incident herpes simplex virus type 2 infections in 2012. PLoS One 10 (1), e114989.

Lu, Y., Cheng, D., Niu, B., Wang, X., Wu, X., Wang, A., 2023. Properties of poly (lactic-co-glycolic acid) and Progress of poly (lactic-co-glycolic acid)-based biodegradable materials in biomedical research. Pharmaceuticals (basel, Switzerland) 16 (3), 454. https://doi.org/10.3390/ph16030454.

Marchi, S., Trombetta, C.M., Gasparini, R., Temperton, N., Montomoli, E., 2017. Epidemiology of herpes simplex virus type 1 and 2 in Italy: a seroprevalence study from 2000 to 2014. J. Prev. Med. Hyg. 58 (1), E27–E33.

Mathew Jr J, Sapra A., 2023. Herpes Simplex Type 2. [Updated 2022 Aug 8]. In: StatPearls [Internet]. Treasure Island (FL): StatPearls Publishing; 2023 Jan-. Available from: https://www.ncbi.nlm.nih.gov/books/NBK554427/.

Modi, S., Van, L., Gewirtzman, A., Mendoza, N., Bartlett, B., Tremaine, A.M., Tyring, S., 2008. Single-day treatment for orolabial and genital herpes: a brief review of pathogenesis and pharmacology. Ther. Clin. Risk Manag. 4 (2), 409–417. https://doi.org/10.2147/tcrm.s1664.

Nair, P.A., Patel, B.C., 2023. Herpes Zoster. [Updated 2022 Sep 5]. In: StatPearls [Internet]. Treasure Island (FL): StatPearls Publishing; 2023 Jan-. Available from: https://www.ncbi.nlm.nih.gov/books/NBK441824/.

Opstelten, W., Eekhof, J., Neven, A.K., Verheij, T., 2008. Treatment of herpes zoster. Can. Fam. Physician 54 (3), 373–377.

Partheniadis, I., Athanasiou, K., Laidmae, I., Heinamaki, J., Nikolakakis, I., 2022. Physicomechanical characterization and tablet compression of theophylline nanofibrous mats prepared by conventional and ultrasound enhanced electrospinning. Int. J. Pharmaceut. 616, 121558 https://doi.org/10.1016/j.ijpharm.2022.121558.

Patil, A., Goldust, M., Wollina, U., 2022. Herpes zoster: a review of clinical manifestations and management. Viruses 14 (2), 192. https://doi.org/10.3390/v14020192.

Romanowski, E.G., Gordon, Y.J., 2001. Effects of diclofenac or ketorolac on the inhibitory activity of cidofovir in the Ad5/NZW rabbit model. Investigative Ophthalmol. Visual Sci. 42 (1), 158–162.

Saleh, D., Yarrarapu, S.N.S., Sharma, S., 2023. Herpes Simplex Type 1. [Updated 2022 Aug 29]. In: StatPearls [Internet]. Treasure Island (FL): StatPearls Publishing; 2023 Jan-. Available from: https://www.ncbi.nlm.nih.gov/books/NBK482197/.

Schiffer, J.T., Corey, L., 2009. New concepts in understanding genital herpes. Curr. Infect. Dis. Rep. 11 (6), 457–464. https://doi.org/10.1007/s11908-009-0066-7.

Shamshina, J.L., Cojocaru, O.A., Kelley, S.P., Bica, K., Wallace, S.P., Gurau, G., Rogers, R. D., 2017. Acyclovir as an ionic liquid cation or anion can improve aqueous solubility. ACS Omega 2 (7), 3483–3493. https://doi.org/10.1021/acsomega.7b00554.

Sill, T.J., von Recum, H.A., 2008. Electrospinning: applications in drug delivery and tissue engineering. Biomaterials 29 (13), 1989–2006. https://doi.org/10.1016/j.biomaterials.2008.01.011.

Sohn, Y.T., Seo, H.O., 2004. Crystal forms of ketorolac. Arch. Pharm. Res. 27 (3), 357–360. https://doi.org/10.1007/BF02980073.

Strasfeld, L., Chou, S., 2010. Antiviral drug resistance: mechanisms and clinical implications. Infect. Dis. Clin. North Am. 24 (2), 413–437. https://doi.org/10.1016/j.idc.2010.01.001.

Strommen, G.L., Pucino, F., Tight, R.R., Beck, C.L., 1988. Human infection with herpes zoster: etiology, pathophysiology, diagnosis, clinical course, and treatment. Pharmacotherapy 8 (1), 52–68. https://doi.org/10.1002/j.1875-9114.1988.tb04066.x.

Swider, E., Koshkina, O., Tel, J., Cruz, L.J., de Vries, I.J.M., Srinivas, M., 2018. Customizing poly(lactic-co-glycolic acid) particles for biomedical applications. Acta Biomater. 73, 38–51. https://doi.org/10.1016/j.actbio.2018.04.006.

Świerzewski, R., Poznański, J., Golankiewicz, B., Zielenkiewicz, W., 2002. NMR investigations of the stacking-like self-association of acyclovir, bromoacyclovir and ganciclovir. J. Mol. Liquids 95 (3), 339–345.

Tunsuriyawong, S., Puavilai, S., 2005. Herpes zoster, clinical course and associated diseases: a 5-year retrospective study at Ramathibodi Hospital. J. Med. Assoc. Thailand = Chotmaihet Thangphaet 88 (5), 678–681.

Villarreal-Gómez, L.J., Cornejo-Bravo, J.M., Vera-Graziano, R., Grande, D., 2016. Electrospinning as a powerful technique for biomedical applications: a critically selected survey. J. Biomater. Sci. Polym. Ed. 27 (2), 157–176. https://doi.org/10.1080/09205063.2015.1116885.

Wang, Y., Qiao, X., Yang, X., Yuan, M., Xian, S., Zhang, L., Yang, D., Liu, S., Dai, F., Tan, Z., Cheng, Y., 2020. The role of a drug-loaded poly (lactic co-glycolic acid) (PLGA) copolymer stent in the treatment of ovarian cancer. Cancer Biol. Med. 17 (1), 237–250. https://doi.org/10.20892/j.issn.2095-3941.2019.0169.

Weng, C.J., Liao, C.T., Hsu, M.Y., Chang, F.P., Liu, S.J., 2022. Simvastatin-loaded nanofibrous membrane efficiency on the repair of Achilles tendons. Int. J. Nanomed. 17, 1171–1184.

Werner, R.N., Ghoreschi, K., 2022. Herpes zoster – prävention, diagnostik und behandlung [herpes zoster-prevention, diagnosis, and treatment]. Der Hautarzt; Zeitschrift Fur Dermatologie, Venerologie, Und Verwandte Gebiete 73 (6), 442–451. https://doi.org/10.1007/s00105-022-04992-9.

Whitley, R.J., 1996. Herpesviruses. In: Baron, S. (Ed.), Medical Microbiology, 4th ed. University of Texas Medical Branch at Galveston.

Whitley, R., Kimberlin, D. W., Prober, C.G., 2007. Pathogenesis and disease. In: Arvin, A., et al. (Eds.), Human Herpesviruses: Biology, Therapy, and Immunoprophylaxis. Cambridge University Press.

Whitley, R.J., Roizman, B., 2001. Herpes simplex virus infections. Lancet (london, England) 357 (9267), 1513–1518. https://doi.org/10.1016/S0140-6736(00)04638-9.

Xue, J., Wu, T., Dai, Y., Xia, Y., 2019. Electrospinning and electrospun nanofibers: methods, materials, and applications. Chem. Rev. 119 (8), 5298–5415. https://doi.org/10.1021/acs.chemrev.8b00593.